10/4-29-91 JSD(1)

UCID- 18987-91

Report to the DOE Nuclear Data Committee

1991

D. A. Resler and R. M. White
Nuclear Data Group
Computational Physics Division

March 1991

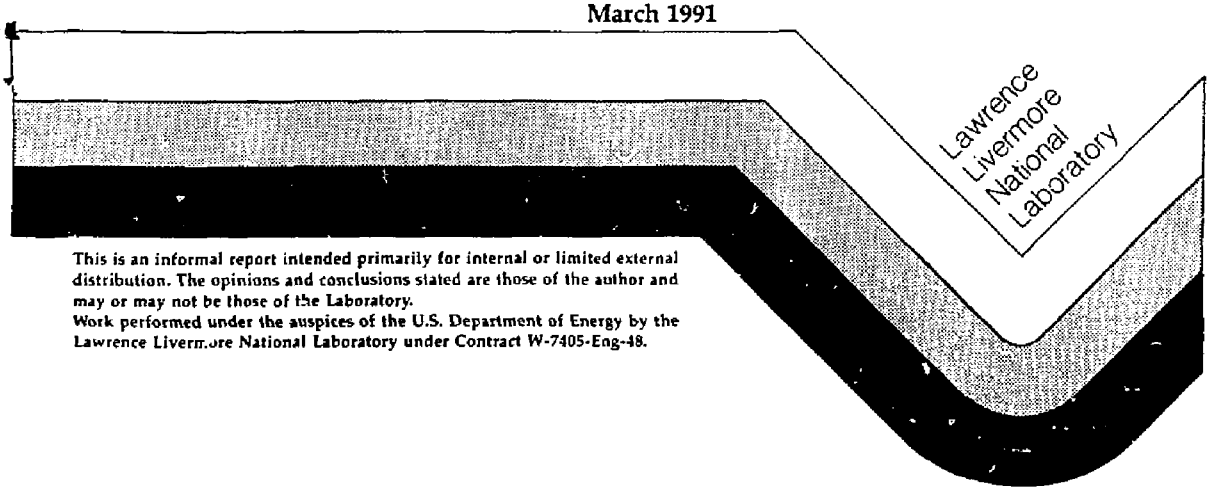

UCID--18987-91

DE91 010909

LAWRENCE LIVERMORE NATIONAL LABORATORY

A. NUCLEAR DATA EVALUATIONS AND CALCULATIONS

1. Charged-Particle Evaluations for Applications (R. M. White and D. A. Resler)

Thermonuclear reaction rates and quantities such as thermally-broadened emission spectra of secondary reaction particles as a function of plasma temperature are essential for the correct modeling of a multitude of problems ranging from fusion energy applications to astrophysics. Of primary interest to fusion applications are the reaction rates of the various isotopes of hydrogen and helium-3. We have finished new evaluations for the $^2H(d,p)^3H$, $^2H(d,n)^3He$, $^3H(d,n)^4He$, $^3He(d,p)^4He$, and $^3H(t,2n)^4He$ reactions from E_{min} to 30 MeV. E_{min} is taken as the energy where the reaction cross section is approximately 10^{-31} barns, a practical limit for many 32-bit computers. These small cross sections at low energies are due to the Coulomb penetrability and require different evaluation techniques than do neutron reactions. However, these low-energy cross sections are important in charged-particle reactions because the average interaction energy in a plasma is also low. The energy range of the cross sections described here amply covers the energies necessary to calculate Maxwellian-averaged reaction rates for plasma temperatures from 100 eV to 1 MeV. The evaluations are based on all published data known to us from 1946 to 1990 and include over 1150 measured data points from over 85 references. While there have been many parameterizations of these reactions and numerous evaluations spanning selected energy regions, we know of no work containing all measurements spanning both this time period and this energy range. A complete bibliographic listing and a detailed description of the evaluation techniques will be presented in a forthcoming LLNL report.

a. $^2H(d,p)^3H$ Evaluation

Our data base for the $^2H(d,p)^3H$ reaction contains 21 references and includes 189 integrated cross section values obtained from a variety of experimental measurements. Figure 1 shows the reference symbols (with the year in brackets) and Fig. 2 shows our evaluation of the $^2H(d,p)^3H$ reaction over the energy region from 350 eV to 200 keV plotted in terms of the astrophysical s-factor with ±3% indicated. One of the principal objectives in carrying out these evaluations is to establish the probable uncertainties (at the 95% confidence level) in the state of knowledge of each of these reactions. In this particular case, while the data appear far more discrepant in the energy region between 350 eV and 200 keV than the ±3% would indicate, the evaluation in this region is based also upon our knowledge of the structure of the ^4He compound system as well as upon numerous measurements at energies greater than 200 keV. The recent high precision measurements of Brown[90] at Los Alamos are in almost perfect agreement with this evaluation which was carried out with and without considering those data.

EB

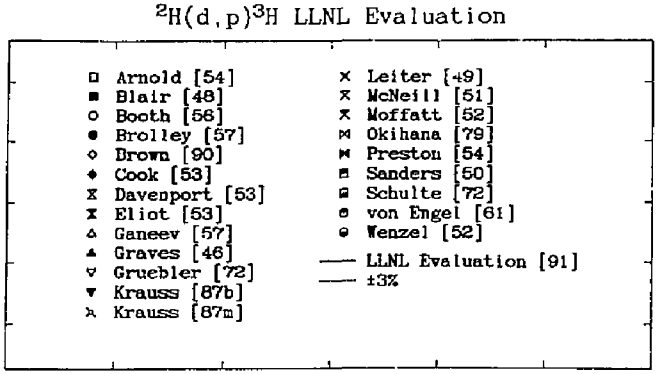

Fig. 1 Reference symbols and authors (with year of publication) for the data base used in the LLNL[91] evaluation of the $^2H(d,p)^3H$ reaction as shown in Fig. 2. A complete bibliographic listing as well as a detailed description of the evaluation techniques used for this reaction will be presented in a forthcoming LLNL report.

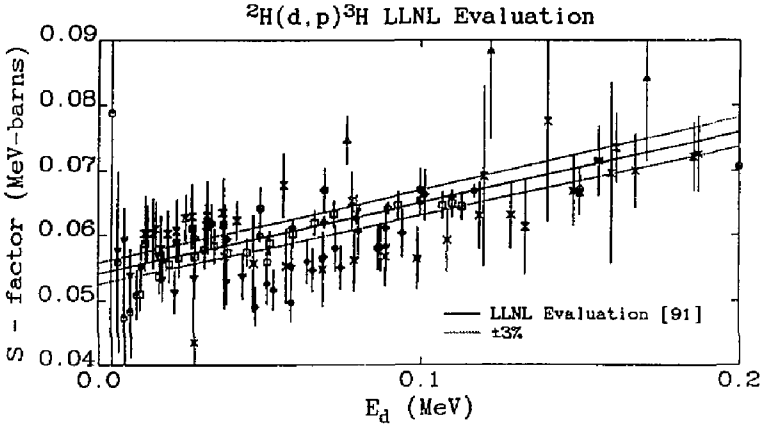

Fig. 2 Plot of the LLNL[91] evaluation of the $^2H(d,p)^3H$ reaction in terms of the astrophysical s-factor as a function of laboratory deuteron energy between 350 eV and 200 keV. The ±3% indicated on the plot represents our estimate of the uncertainty in the evaluation (at the 95% confidence level). While the $^2H(d,p)^3H$ data are most discrepant in the energy region below 200 keV, the knowledge of the structure of the ^4He compound system, as well as the data base above 200 keV, give us strong confidence in this evaluation. The recent high precision measurements of Brown[90] at Los Alamos are in almost perfect agreement with this evaluation which we made both with and without considering those data.

b. $^{2}H(d,n)^{3}He$ Evaluation

Our data base for the $^{2}H(d,p)^{3}H$ reaction contains 21 references and includes 190 integrated cross section values. Figure 3 shows the reference symbols and Fig. 4 shows our evaluation of the $^{2}H(d,n)^{3}He$ reaction from 350 eV to 200 keV plotted in terms of the astrophysical s-factor with ±3% indicated. In this reaction, several measurements in the energy range below 100 keV might indicate that the evaluation should have the slope shown here but be lowered by 6-8%. However, similarly to the $^{2}H(d,p)^{3}H$ reaction, knowledge of the structure of the compound ^{4}He system, as well as the data base above 200 keV, give us strong confidence in this evaluation. As in the case of the $^{2}H(d,p)^{3}H$ reaction, the recent Los Alamos measurement of the $^{2}H(d,n)^{3}He$ reaction is in excellent agreement with our evaluation which was carried out with and without considering their data.

c. $^{3}H(d,n)^{4}He$ Evaluation

Our data base for the $^{3}H(d,n)^{4}He$ reaction contains 19 references and includes 366 integrated cross section values. Figure 5 shows the reference symbols and Figs. 6 and 7 show our evaluation of the $^{3}H(d,n)^{4}He$ reaction from 300 eV to 200 keV plotted in terms of the astrophysical s-factor and cross section, respectively, with ±2% indicated. For the energy range shown, the evaluation is based on a single-level R-matrix fit to all of the available data except for three data sets whose shape and normalization are not consistent with the majority of the other measurements. Many R-matrix calculations were performed under a variety of fitting ranges and using various subsets of the main data set. The conclusion was that all of the results fell within the ±2% band indicated around the final evaluation. The Los Alamos one and two-level fits to this reaction also fall within this ±2% band. Details of the R-matrix calculations will be presented in a forthcoming LLNL report.

d. $^{3}He(d,p)^{4}He$ Evaluation

Our data base for the $^{3}He(d,p)^{4}He$ reaction contains 17 references and include 262 integrated cross section values. Figure 8 shows the reference symbols and Figs. 9 and 10 show our evaluation of the $^{3}He(d,p)^{4}He$ reaction from 1.25 keV to 1 MeV plotted in terms of the astrophysical s-factor and cross section, respectively, with ±8% indicated. Of the five reactions evaluated in this work, the data sets for this reaction are the most discrepant. The absolute values disagree by more than the experimenters' quoted errors. However, except for two full data sets and the low-energy portion of two other data sets, the shapes are in good agreement. Over the energy range from 1.25 keV to 800 keV, the evaluation is based on a single-level R-matrix fit to all of the available data except for the data which were discrepant in shape. As with the $^{3}H(d,n)^{4}He$ reaction, many R-matrix calculations were performed under a variety of conditions.

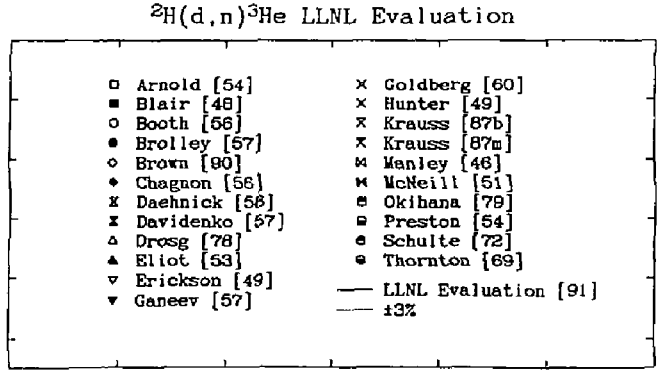

Fig. 3 Reference symbols and authors (with year of publication) for the data base used in the LLNL[91] evaluation of the ^{2}H(d,n)^{3}He reaction as shown in Fig. 4. A complete bibliographic listing as well as a detailed description of the evaluation techniques used for this reaction will be presented in a forthcoming LLNL report.

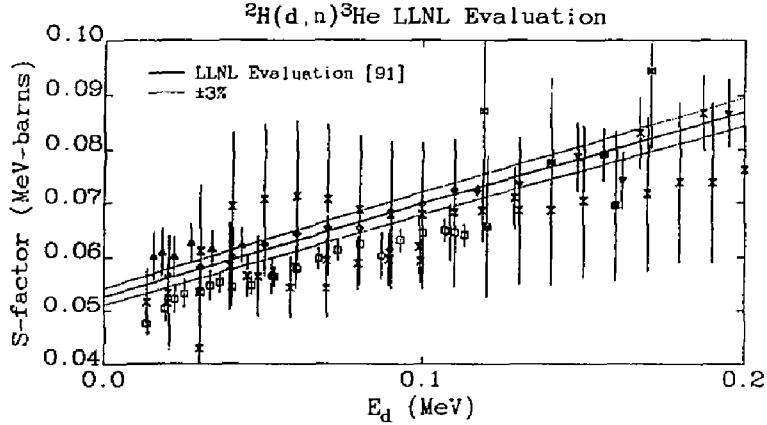

Fig. 4 Plot of the LLNL[91] evaluation of the ^{2}H(d,n)^{3}He reaction in terms of the astrophysical s-factor as a function of laboratory deuteron energy between 350 eV and 200 keV. The ±3% indicated on the plot represents our estimate of the uncertainty in the evaluation (at the 95% confidence level). In this reaction, several measurements in the energy range below 100 keV might indicate that the evaluation should have the slope shown here but be lowered by 8-10%. However, similarly to the ^{2}H(d,p)^{3}H reaction, knowledge of the structure of the ^{4}He compound system, as well as many measurements above 100 keV, indicate that there should be no significant curvature in the astrophysical s-factor in this energy region.

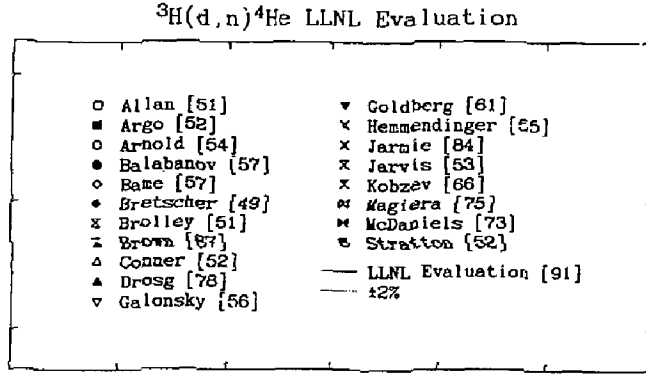

Fig. 5 Reference symbols and authors (with year of publication) for the data base used in the LLNL[91] evaluation of the ^{3}H(d,n)^{4}He reaction as shown in Figs. 6 and 7. A complete bibliographic listing as well as a detailed description of the evaluation techniques used for this reaction will be presented in a forthcoming LLNL report.

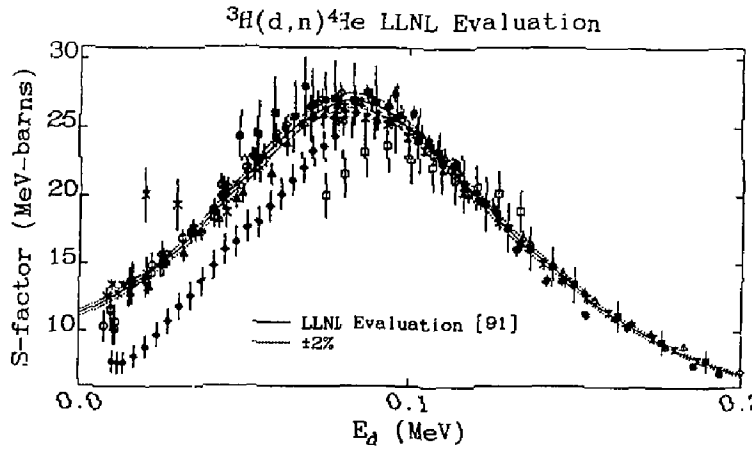

Fig. 6 Plot of the LLNL[91] evaluation of the ^{3}H(d,n)^{4}He reaction in terms of the astrophysical s-factor as a function of laboratory deuteron energy between 300 eV and 200 keV. The ±2% indicated on the plot represents our estimate of the uncertainty in the evaluation (at the 95% confidence level). With the exception of three data sets whose shape and normalization are not consistent with the majority of other measurements, the ^{3}H(d,n)^{4}He data in this region are very consistent.

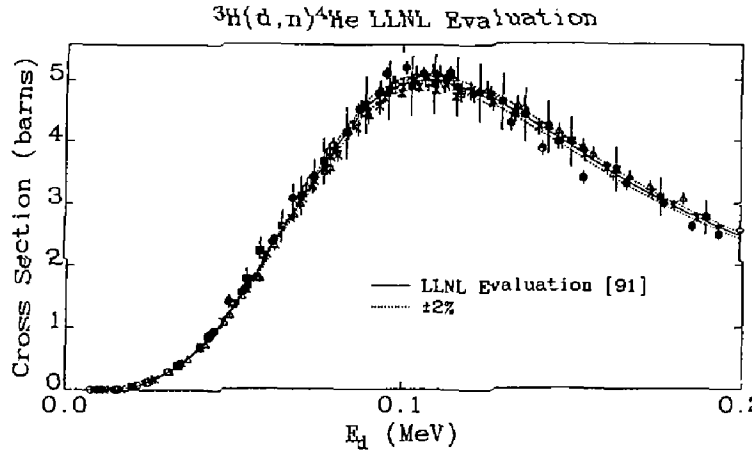

Fig. 7 Plot of the LLNL[91] evaluation of the ^{3}H(d,n)^{4}He reaction cross section from 300 eV to 200 keV with the three discrepant data sets removed. The evaluation procedures we used on the data base for this reaction and comparing our evaluation with other recent evaluations leads us to condude that, unless some significant new experimental technique is developed, our estimate of the ±2% uncertainly for this reaction is unlikely to be reduced.

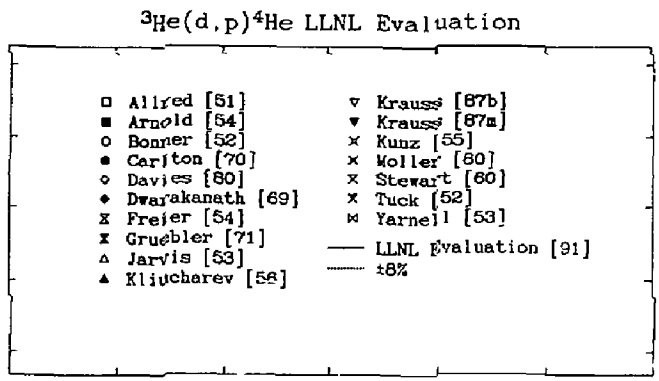

Fig. 8 Reference symbols and authors (with year of publication) for the data base used in the LLNL[91] evaluation of the ^{3}He(d,p)^{4}He reaction as shown in Figs. 9 and 10. A complete bibliographic listing as well as a detailed description of the evaluation techniques used for this reaction will be presented in a forthcoming LLNL report.

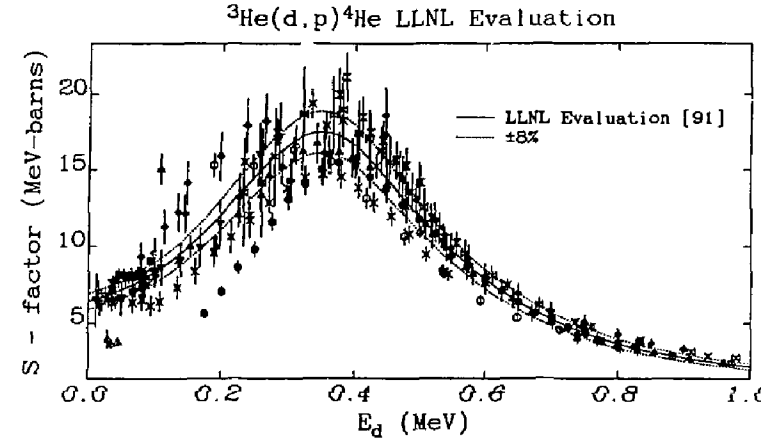

Fig. 9 Plot of the LLNL[91] evaluation of the ^{3}He(d,p)^{4}He reaction in terms of the astrophysical s-factor as a function of laboratory deuteron energy between 1.25 keV and 200 keV. The ±8% indicated on the plot represents our estimate of the uncertainty in the evaluation (at the 95% confidence level). While the data are discrepant in magnitude by more than the quoted errors, the shapes are in good agreement except for two full data sets and the low-energy portion of two other data sets.

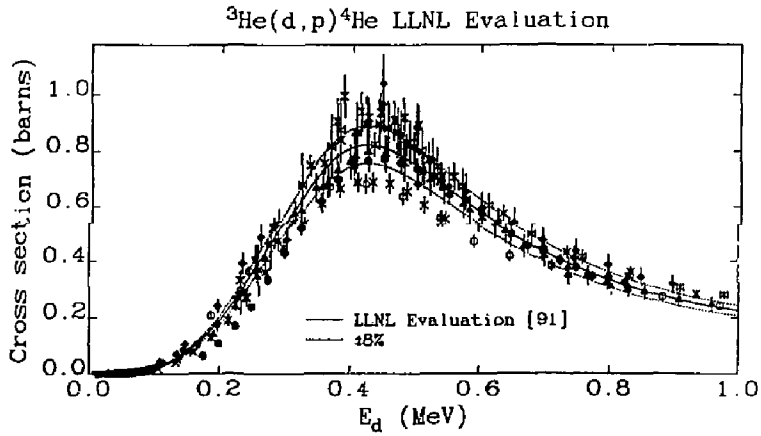

Fig. 10 Plot of the LLNL[91] evaluation of the ^{3}He(d,p)^{4}He reaction cross section from 1.25 keV to 200 keV as a function of laboratory deuteron energy. The evaluation is based on a single-level R-matrix fit to the data as is described in the text. Because of the discrepant nature of the data we have assigned ±8% as the uncertainty in the evaluation (at the 95% confidence level).

The best fit was obtained by simultaneously allowing the data set normalizations to change while fitting with the single-level R-matrix calculation. Since there were several data sets whose overall normalizations were more discrepant than the quoted errors and since it was not obvious why one measurement might be better than another, it was decided that the best one could do was assume that, on the average, the overall normalization of the entire data base was correct. Therefore, the individual data set normalizations were allowed to change subject to the constraint that the average normalization was unity.

e. $^3H(t,2n)^4He$ Evaluation

Our data base for the $^3H(t,2n)^4He$ reaction contains 6 references and includes 117 integrated cross sections values. By the nature of the reactants, this reaction is difficult to measure and experimental data extend to only 2.2 MeV. Figure 11 shows the $^3H(t,2n)^4He$ data up to 1 MeV and our evaluation from 500 eV to 1 MeV plotted in terms of the astrophysical s-factor with ±8% indicated. Our evaluation comes from a least-squares cubic spline fit to all the data in this region. There is a clear change in slope of the low energy data independent of any one data set. At higher energies, the evaluation follows the projection of Govorov[62] and the measurement at 1.9 MeV of Jarmie[58]. Because there exist no measured data above 2.2 MeV some estimate had to be made of the probable shape and magnitude of the high energy $^3H(t,2n)^4He$ reaction cross section. Figure 12 shows the high energy evaluation of the $^3H(t,2n)^4He$ reaction in comparison with the other four reactions.

2. Advanced Modeling of Reaction Cross Sections for Light Nuclei (D. A. Resler, S. D. Bloom, and S. A. Moszkowski)

Over the last several years we have put together a system of codes for modeling reaction cross sections for light nuclei. The technique involves starting with an effective nucleon-nucleon interaction. In general, nuclear reaction cross sections for light projectiles (n, p, d, t, ^3He, α) of low-energy ($E \leq 20$ MeV) incident on light nuclei ($A \leq 20$) are dominated by isolated and overlapping resonance behavior. These resonances are due to the structure of the compound nucleus. By starting with an effective nucleon-nucleon interaction, the properties of the compound nuclear structure can be obtained through the nuclear shell model. This structure information can then be transformed into the required input to an R-matrix code for the calculation of reaction cross sections. Because of the fundamental nature of the calculations, i.e., starting from a nucleon-nucleon interaction, if the method can be used to accurately calculate reaction cross sections where one has data to compare with (such as the evaluations presented in the previous section), then the method can be used with confidence where little or no data exist (such as $d+^6Li$).

In general, the model spaces needed for the shell model calculations require excitations for which current effective nucleon-nucleon interactions do not work properly. In an effort to ameleorate these problems, we are developing a new effective nucleon-nucleon

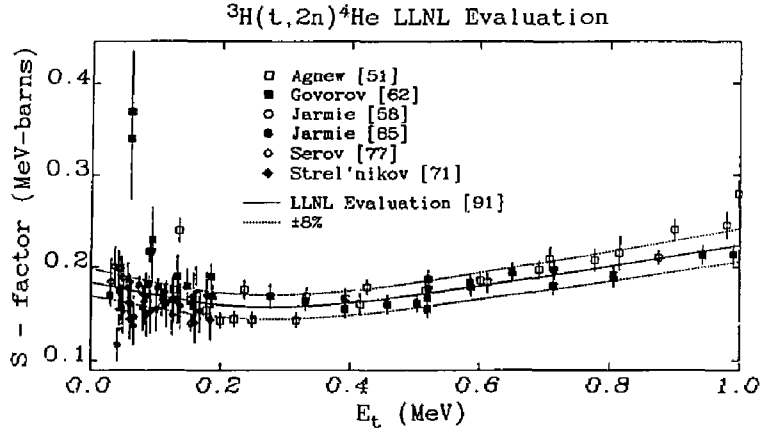

Fig. 11 Plot of the LLNL[91] evaluation of the ^{3}H(t,2n)^{4}He reaction in terms of the astrophysical s-factor as a function of laboratory deuteron energy between 500 eV to 1 MeV. The ±8% indicated on the plot represents our estimate of the uncertainty in the evaluation (at the 95% confidence level). Also shown are the reference symbols and authors (with year of publication) for the data base. A complete bibliographic listing as well as a detailed description of the evaluation techniques used for this reaction will be presented in a forthcoming LLNL report.

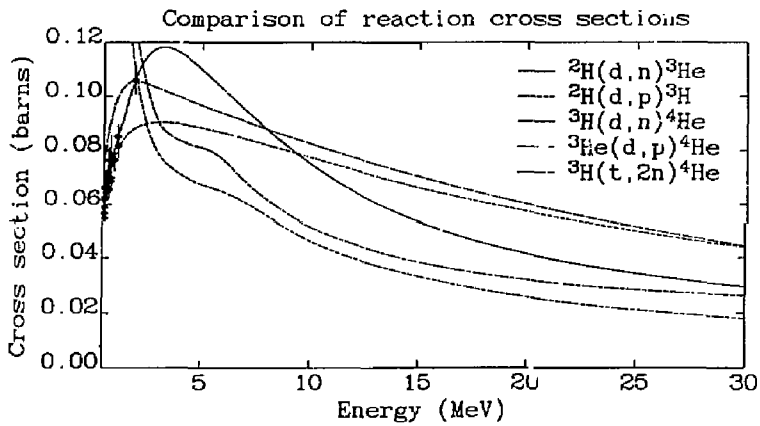

Fig. 12 Comparison of the cross sections for the five reactions considered in this work. Because there exist no measured data above 2.2 MeV for the ^{3}H(t,2n)^{4}He reaction some estimate has to be made of the probable shape and magnitude above 2.2 MeV. This comparison shows that what we have chosen is not unreasonable in light of the other reactions.

interaction for use in large model spaces and additionally to correctly determine basic properties of nuclei and nuclear matter (i.e., binding energies/nucleon and saturation) and to reduce to a Skyrme-like (Hartree-Fock) interaction in the short range limit. Our phenomenological interaction consists of three components (see Figure 13), each containing four parts: (1) a potential strength V, (2) a gaussian radial form factor, e^{-r^2/a^2}, (3) non-locality (gaussian in momentum space), $e^{-p^2c^2}$, and (4) a density-dependent term. The longest range (r) component is assumed to be attractive, density independent, and local (c=0). This component is constructed to look like the one pion exchange potential (OPEP). It is also this component which leads to the extra clustering that one finds in ^{4}He. The second component is of shorter range and is assumed to be attractive, density independent, and non-local. The third component is of still shorter range, repulsive, density dependent, and non-local. The last two components look much like a surface delta interaction and are required for saturation. The parameters of our interaction are being determined by least-squares techniques using the global constraints (binding energies/nucleon and saturation) for ^{4}He, ^{16}O, and nuclear matter. We have evidence that such an interaction does much to alleviate the problems previously seen in calculations performed in large model spaces.

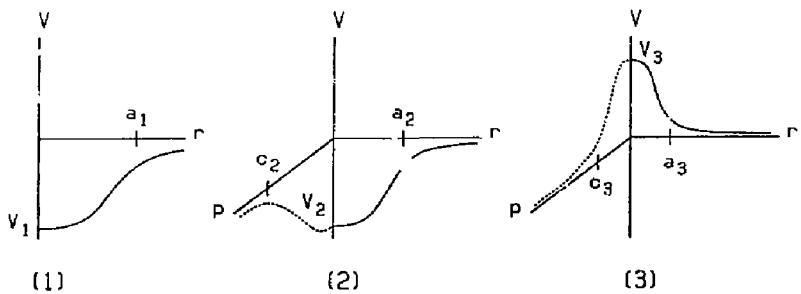

Fig. 13 Diagram of the three components being employed in the present quest for an improved nucleon-nucleon interaction. The first component is constructed to look like a one pion exchange potential and leads to the extra clustering that one finds in ^{4}He. The second and third components look much like a surface delta interaction and are required for saturation. Refer to the text for more details.

3. TDF—A Processed File for Thermonuclear Applications (S. I. Warshaw and R. M. White)

We have created a processed thermonuclear data file, TDF, and the computer routines, written in standard FORTRAN, with which to read this file. The TDF file contains information calculated from our evaluations such as Maxwellian-averaged reaction rates as a function of reaction and plasma temperature, the Maxwellian-averaged average energy of the interacting particles as well as the same quantities for the secondary reaction products.

Also included are routines which provide thermally-broadened spectral information for the secondary reaction products. These routines are useful for either deterministic or Monte Carlo calculations and special emphasis has been placed on making them easy to use. Documentation and availability of TDF and the routines which access it will be available to the user community by early summer 1991.

4. Evaluation of (n,2n) reactions on Isotopes of Y and Zr (M. H. MacGregor and G. Reffo)

We have carried out an evaluation of neutron-induced reactions on the isotopes $^{87,88,89}Y$ and $^{88,89,90}Zr$. These isotopes have been extensively studied in previous evaluations, and they serve as a valuable benchmark. ^{89}Y and ^{90}Zr are stable and there exists experimental information on these isotopes. The other isotopes are unstable and there exists almost no experimental information about them. Hence their cross sections must be obtained by calculational means. These isotopes occur at or near the magic neutron number N=50, which means that the nuclear systematics are varying rapidly in this region, and comprehensive studies must be made in order to extract the proper level densities. We used the Livermore version of the ENEA code set IDA for these calculations.

To calculate all the important particle decay channels, it is necessary to include 35 isotopes of Br, Kr, Rb, Sr, Y and Zr in the evaluation. The neutron resonances for these and neighboring nuclei were statistically analyzed with the IDA module ESTIMA in order to obtain the best values for the Fermi gas constant "a". The variation of "a" with neutron number is shown in Fig. 14, where the influence of the magic number N=50 is clearly apparent. The low-lying levels in these nuclei were analyzed with the IDA module AMLETO in order to obtain the correct nuclear "temperatures". These temperatures are combined with the Fermi gas constants to produce a self-consistent set of Gilbert and Cameron level densities for use in the Hauser-Feshbach formalism. A variety of optical models were also studied in order to obtain the best set of transmission coefficients for use in the Hauser-Feshbach calculations. Intercomparisons between the IDA module PENELOPE and the LLNL ALICE code were made to evaluate pre-equilibrium effects, which have a strong influence on the (n,2n) cross sections. The IDA module POLIFEMO was used to provide the width fluctuation corrections to the Hauser-Feshbach calculations. In the evaluation, the IDA nuclear density and temperature parameters were first obtained as described above, and were then adjusted so as to give the best fits to the available experimental data. These optimized parameters were used to calculate the reactions where no experimental data exist. Calculations involving isomeric-state target nuclei are still in progress. Figures 15, 16, and 17 show comparisons of our calculations for the (n,2n) cross sections of $^{87,88,89}Y$. In Figs. 15 and 16, where experimental data exist, both evaluations are in good agreement. However, in Fig. 17, where no experimental data are available to serve as normalizations, our evaluation differs by roughly 20% from other calculations. We believe this indicates the general level of accuracy that can be expected from theoretical nuclear modeling calculations in this mass region.

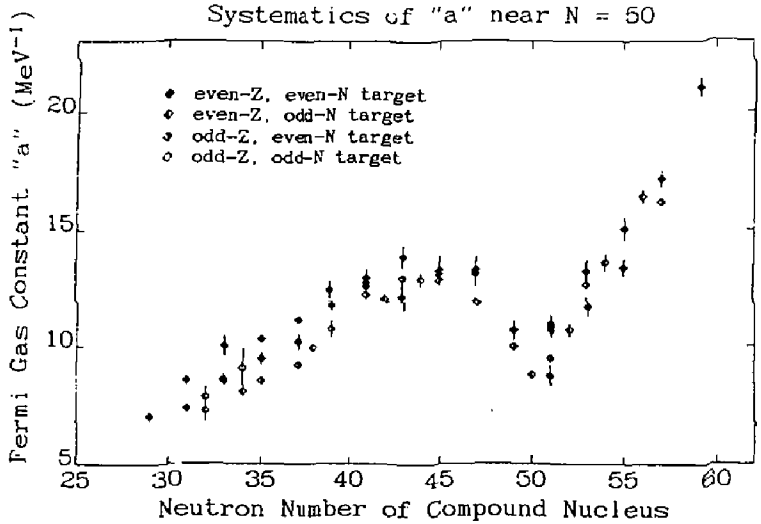

Fig. 14 Systematics of the Fermi gas constant "a" as a function of neutron number near N=50. The influence of the magic number N=50 is clearly apparent. These systematics were obtained from an analysis of neutron resonances using the IDA module ESTIMA.

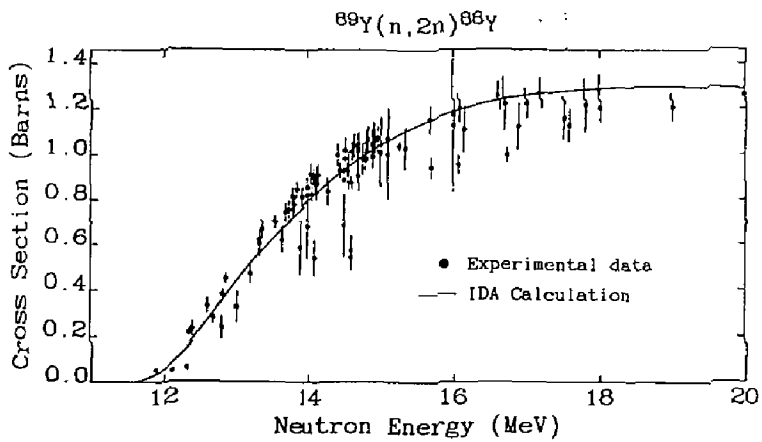

Fig. 15 Comparison of the IDA calculation to the experimental data for the $^{89}Y(n,2n)^{88}Y$ reaction. Details of the IDA calculation are given in the text.

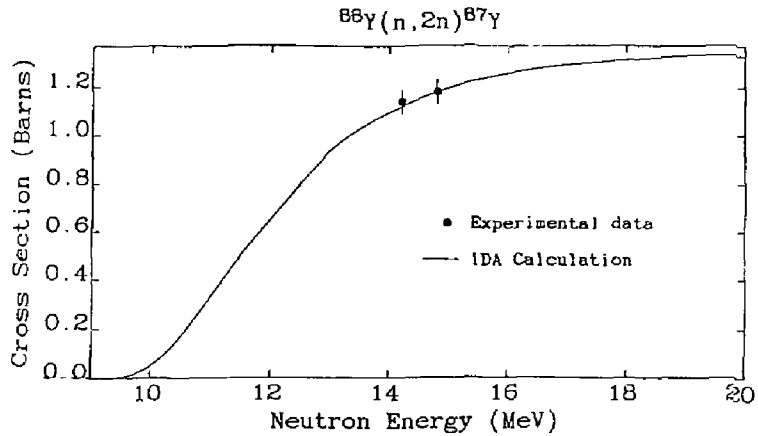

Fig. 16 Comparison of the IDA calculation to the two experimental data points for the $^{88}Y(n,2n)^{87}Y$ reaction. Details of the IDA calculation are given in the text.

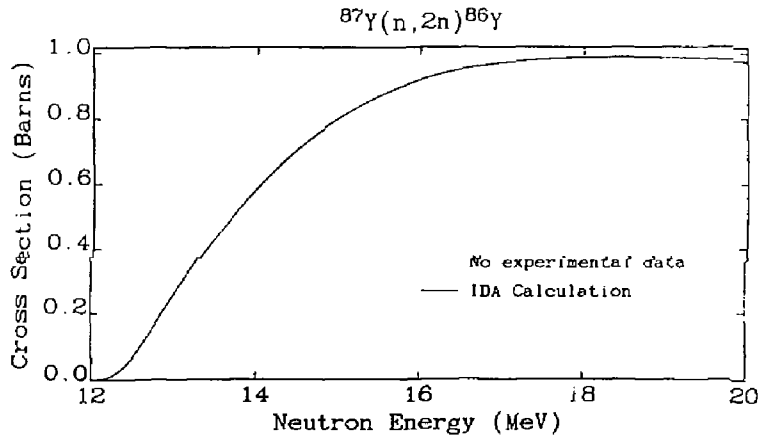

Fig. 17 Shown is the IDA calculation for the $^{87}Y(n,2n)^{86}Y$ reaction. Since there exist no experimental data to serve as normalizations, our evaluation differs by roughly 20% from other calculations and we believe this indicates the general level of accuracy that can be expected from modeling in this mass region.

5. Extension of the LLNL Evaluated Nuclear Data Base (ENDL) to 30 MeV (M. Blann and T. Komoto)

We have been extending our evaluated nuclear data base for reactions induced by neutrons up to 30 MeV. The data base will be suitable for use in transport calculations, and so must give output on an exclusive basis. We have thus far modified the ALICE code to calculate n, p, and α particle spectra with up to three successive particle emission channels (27 channels) on an exclusive basis, giving results in a format suitable for immediate inclusion into the database. We must calculate the contributions from reactions which may emit more than three n, p, or α particles at the higher energies of interest, to see if four particle exclusive reactions need to be included in the calculated data file.

For fissile nuclei we have completed code modifications to follow exclusive fission and non-fission channels up to and including third-chance fission. We have decided on algorithms for treating neutron spectra for fourth and fifth chance fission, to be encoded shortly. Additionally the Bohr-Wheeler fission treatment is being replaced by tabular fission probabilities based closely on experimental results where available.

The fission neutron spectra are now encoded to use the Watt distribution, using neutron multiplicity algorithms developed by R. J. Howerton. Prefission precompound plus compound neutrons are added to the postfission neutron spectra. The precompound plus compound channels determine the cross section vs. excitation used as input into the Howerton algorithms. We believe that reliance on experimental fission probabilities using proven neutron multiplicity algorithms through nuclear modeling will provide a reliable extrapolation to the 30 MeV incident neutron energy regime.

6. Calculated Kerma Values (R J. Howerton)

Kerma values have been calculated from the January 1991 version of LLNL's Evaluated Neutron Data Library (ENDL). This effort is in support of the IAEA's Coordination Research Program (CRP) on Nuclear Data Needed for Neutron Therapy. Generally, the kerma for a neutron-induced reaction is defined to be the energy available from the reaction (E_n + Q) less the energy carried off by secondary neutrons and photons (E_n is the incident neutron energy and Q is the Q-value for the reaction). The kerma for a material is then obtained by summing the kermas of the individual reactions, properly weighted by isotopic or elemental abundance in the case of composite materials.

Explicit energy distributions for all secondary particles from all neutron-induced reactions are routinely entered into the LLNL ENDL data files. With these quantities, it is possible to insure energy conservation between neutron interaction and neutron-induced gamma-ray production data and to calculate average energy deposits for all secondary particles. The tolerance for energy conservation in ENDL is currently 5% or 100 keV, whichever is less.

The kerma factors are presented in the form of histograms for 175 neutron energy groups commonly used at LLNL for the isotopes and naturally occurring elemental mixtures of isotopes. For composite materials, a subset of these groups is required that eliminates neutron energies below the molecular binding energies of the materials. At these energies, different physical mechanisms than those associated with nuclear reactions are required. The histogram form was selected because it is impractical to tabulate kerma factors on a linear basis and because the kerma factors change slowly enough over the groups that linear interpolation will yield values that are within the uncertainties of the basic data from which they are calculated. Since the calculated kerma factors were derived from the evaluated data in ENDL, any errors in the kerma factors are due to errors in the evaluated library.